Chapter 1

Advanced Membrane Material from Marine Biological Polymer and Sensitive Molecular-Size Recognition for Promising Separation Technology

Keita Kashima and Masanao Imai

Additional information is available at the end of the chapter

http://dx.doi.org/10.5772/50734

1. Introduction

Membranes from biological polymers are anticipated practical application as biocompatible materials in separation technology. Biological polymers produced from bioresources are expected to be environmentally compatible polymers and to have great potential as alternatives to various artificial polymers produced from petroleum.

The application of membrane separation in the food industry, medical devices, and water treatment has attracted the attention of biochemical engineering. Membrane separation processes effectively reduce energy cost and CO_2 production. In addition, interest in using natural materials has increased, due to their biocompatibility and their lack of environment load upon disposal. Biopolymer membranes made of cellulose, [1-2], gelatin [3], and chitosan [4] have been anticipated for application in biocompatible separation processing.

1.1. Membrane Desalination

Desalination technology grows exponentially to support water supply from sea water. Today, three billion people around the world have no access to clean drinking water. By 2020, there will be a worldwide 17% short of fresh water needed to sustain the world population. Moreover, 1.76 billion people live in areas already facing a high degree of water stress [5-6].

Generally, desalination can be categorized into two major types: (1) phase-change/thermal process and (2) membrane-based process. Examples of the phase-change process include

multi-stage flash, multiple-effect boiling, vapor compression, freezing humidification/dehumidification, and solar stills. Membrane-based processes include reverse osmosis (RO), nanofiltration (NF), ultrafiltration (UF), membrane distillation (MD), and electrodialysis (ED) [7]. Membrane separation technology for desalination is expected to reduce energy consumption.

1.1.1. Artificial Polymer Membrane for Desalination

Previous studies on membrane desalination are listed in Table 1. Various artificial polymers exhibited excellent capability in separation engineering and practical application for desalination, dialysis, and water treatment [8-10].

Authors	Year	Material	Desalination method	Rf.
Hsu, S. T. et al.	2002	PTFE	MD	8
Haddad, R. et al.	2004	Cellulose	NF	18
Peng, P. et al.	2005	PVA/PEG	MD	9
Gazagnes, L. et al.	2007	Ceramic	MD	10
Miao, J. et al.	2008	Chitosan Polysulfone	NF	16
Padaki, M. et al.	2011	Chitosan Polypropylene	NF	17
Zhang, S. et al.	2011	Cellulose	FO	19
Papageorgiou, S. K. et al.	2012	Alginate	Photocatalytic UF	14

MD: Membrane distillation, NF: Nanofiltration, FO: Forward osmosis, UF: Ultrafiltration
PTFE: Polytetrafluoro ethylene, PVA: Polyvinyl alchohol, PEG: Polyethylene glycol

Table 1. Various membranes for desalination.

1.1.2. Biological Polymer Membrane

Alginate is a typical marine biopolymer used as a fouling model in the desalination field [11-12]. Recently, the high performance of desalination of the alginate membrane has been expected to provide highly efficient desalination because sensitive molecular screening characteristics of the alginate membrane have been demonstrated [13]. In addition, alginate-based materials have been developed as support for photocatalysts. Papageorgiou et al. pioneered a hybrid photocatalytic/ultrafiltration process for treating water containing toxic organic compounds [14].

Chitosan has often been investigated for application in desalinating marine biological polymers. Chitosan membrane has strong antibacterial activity in a higher deacetylation degree

http://dx.doi.org/10.5772/50734

[15]. N,O-carboxymethyl chitosan and polysulfone composite membrane cross-linked with epichlorohydrin was recently developed [16].

At 293K and 0.40 MPa, the membrane rejected 90.4% of the Na_2SO_4 solution (1000mg L^{-1}) while the permeate flux was 7.9 kg m^{-2} h^{-1} (Na_2SO_4). In contrast, the membrane rejected 27.4% of the NaCl solution while the permeate flux was 10.8 kg m^{-2} h^{-1} (NaCl). Polypropylene supported chitosan NF-membrane has also demonstrated good desalination ability in acidic pH [17].

Haddad et al. indicated that cellulose acetate nanofiltration (NF) could be adapted to desalination processes [18]. Cellulose ester membrane was also investigated in forward osmosis (FO) for desalination [19]. Forward osmosis has been applied worldwide in recent years as a novel alternative desalination technology for producing fresh water [20].

2. Alginates

Alginic acid is abundantly produced by marine biological resources, especially brown seaweed. The first description of alginate as a preparation of "algic acid" from brown algae was provided and demonstrated by British chemist E. C. C. Stanford, with a patent dated 12 January 1881 [21]. In 1896, A. Krefting successfully prepared a pure alginic acid. Kelco Company began commercial production of alginates in 1929 and introduced milk-soluble alginic acid as an ice cream stabilizer in 1934 [22].

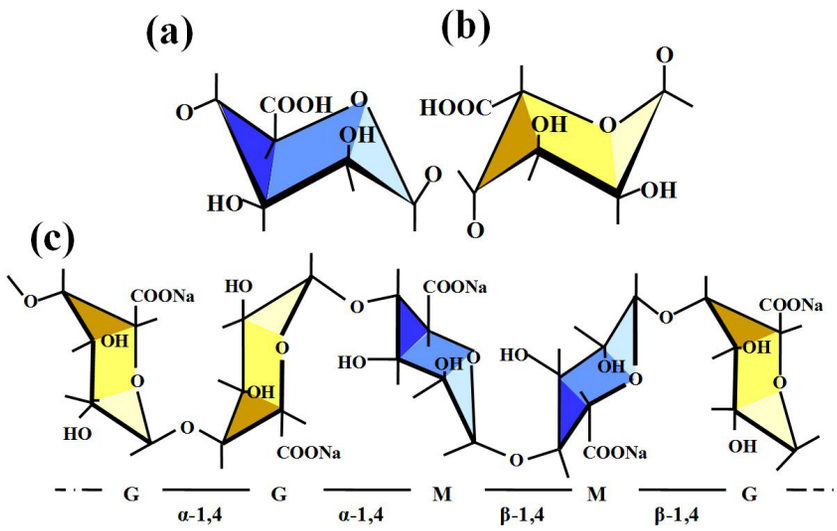

Figure 1. Alginate composition. (a) β-D-mannuronic acid. (b) α-L-guluronic acid. (c) Structural formula of sodium alginate molecule.

Alginates have been conventionally applied in the food industry as thickeners, suspending agents, emulsion stabilizers, gelling agents, and film-forming agents [23].

Sodium alginate is a typical hydrophilic polysaccharide. It consists of a linear copolymer composed of two monomeric units, 1,4-linked β-D-mannuronic acid (Figure 1a) and α-L-guluronic acid (Figure 1b), in varying proportions. These two uronic acids have only minor differences in structure, and they adopt different chair conformations such that the bulky carboxyl group is in the energetically favored equatorial position [24].

The physical properties (e.g., viscosity and mean molecular weight) of sodium alginate are very susceptible to physicochemical factors (e.g., pH and total ionic strength). At near-neutral pH, the high negative charge of sodium alginates due to deprotonated carboxylic functional groups induces repulsive inter- and intra-molecular electrostatic forces. The change of ionic strength in a sodium alginate aqueous solution has a significant effect, especially on the polymer chain extension [25-27].

2.1. Chemical Formation

An alginate molecular chain was constructed using three types of polymeric block: homopolymeric blocks of mannuronic acid (M-M), guluronic acid (G-G), and blocks with an alternating sequence in varying proportions (M-G) [28] (Figure 1c).

The M-M block consists of 1e→4e linked β-D-mannuronic acid chains with the monosaccharide units in a $^4C_1$ chair conformation. Regions in which β-D-mannuronic acid predominates have been predicted to form an extended ribbon structure, analogous to cellulose [29].

The G-G block is composed of 1→4 diaxially linked α-L-guluronic acid residues in a $^1C_4$ chair conformation. It forms a buckled chain [30]. The molecular construction of the G-G block has been confirmed experimentally by X-ray diffraction analysis of the partial hydrolysis products of alginate. The mass fraction of these blocks is basically derived from a natural species of brown algae. At present, the production of new tailor-made alginates has been prompted by the availability of C-5 epimerases, which facilitate extremely efficient tuning of both composition and physicochemical properties of the polysaccharide. In particular, the epimerase AlgE4, which enables the conversion of M-M blocks into alternating sequences in a processive mode of action [31], has provided new alginates with interesting properties. In this respect, besides the remarkable increase in syneresis displayed by the AlgE4 treated samples, a much higher stability of the gel is directly correlated with the presence of long alternating sequences [32-33].

2.2. Gelling Ability

Sodium alginate rapidly forms a gel structure with the presence of divalent cations such as Ca^{2+}, resulting in a highly compacted gel network [34]. Spherical gel particles of calcium alginate are often investigated and applied as a carrier of immobilized enzyme [35], a drug delivery capsule [36], a carrier of entrapped living cells [37-38], and a food supplement [39]. However, the formation of the alginate membrane has not been investigated as much.

http://dx.doi.org/10.5772/50734

The basic ability of alginate to gel is related to its specific ion-binding characteristics [40]. The variation in gel strength has been analyzed in terms of modes of binding of cation by the various block structures that occur within the alginate molecular chain. Experiments involving equilibrium dialysis of alginate have demonstrated that the selective binding of certain alkaline earth metal ions (e.g., strong and cooperative binding of Ca relative to Mg) increases markedly with increasing content of G-G block in the chains. M-M block and M-G block had almost no selectivity [41]. Regions of homopolymeric blocks of α-L-guluronic acid chelate the alkaline earth metal ions because of the spatial arrangement of the ring and hydroxyl oxygen atoms, and thus create a much stronger interaction [24]. These homopolymeric blocks of α-L-guluronic acid junction zones are constructed mainly of a cross-linked area called an "Egg-box," where the Ca^{2+} ions are located as the "Egg" components [42] (Figure 2). NMR studies of lanthanide complexes of related compounds suggested a possible binding site for Ca^{2+} ions in a single alginate chain [43].

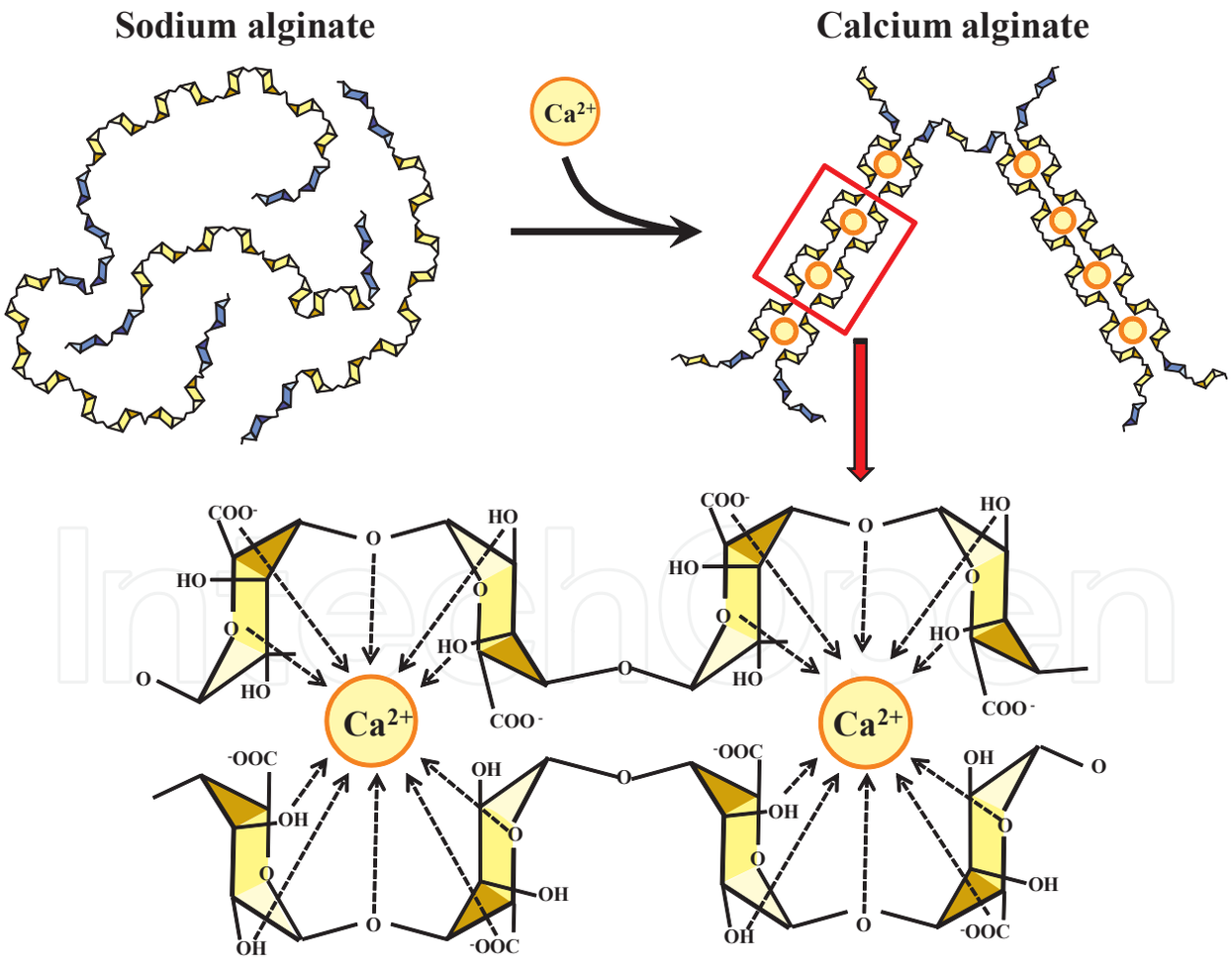

Figure 2. Gelation of homopolymeric blocks of α-L-guluronic acid junction with calcium ions. Binding of divalent cations by alginate: the "Egg-box" model.

3. Membrane Preparation

Many kinds of biopolymer membrane have been utilized and developed in food and biological applications. In general, biopolymer membrane was prepared by casting (e.g., cellulose acetate) [44] and chitosan [45]). Spherical gel particles of sodium alginate have often been investigated and applied. However, the formation of alginate membrane has been less investigated. This section provides a general description of the preparation of various alginate membranes.

3.1. Previous Studies on Membrane Preparation

In recent years, alginate membranes have been investigated in diverse ways (e.g., pervaporation, immobilized cell reactor, and ultrafiltration). Previous studies on alginate membrane are listed in Table 2. Teixeira et al. prepared yeast-cell-occupied calcium alginate membrane [46]. Zhang and Franco prepared a calcium alginate membrane for measuring effective diffusivities using the diffusion-cell technique [47]. Grassi et al. determined the drug diffusion coefficient in a calcium alginate membrane [48]. Alginate membrane prepared by low concentration cross-linker needed support matrix (e.g. glass fiber filter) to maintain flat membrane [49].

3.1.1. Cross-linker

Calcium chloride is basically used as a cross-linker in many investigations of calcium alginate membranes. Calcium sulphate and calcium acetate have also been used as cross-linkers for calcium alginate membrane preparation [23, 50-51]. Other cations (Ba^{2+}, Zn^{2+}) have been used as cross-linkers for preparing alginate membrane [49, 51-52]. Barium chloride provided more improved stability than calcium chloride [49]. Zinc acetate can cause denser cross-linking and less selectively than calcium used with sodium alginate [51].

Sodium alginate membrane cross-linked by glutaraldehyde was applied for acetic acid separation from acetic acid aqueous solution. The membrane was also applied for separating isopropanol from its aqueous solution [53]. Experimental evidence from IR spectroscopy, wide angle X-ray diffractometry, and swelling measurements enabled characterization of the reaction between sodium alginate and glutaraldehyde. The aldehyde groups increased with increasing glutaraldehyde content in the reaction solution [54].

Kalyani et al. prepared a sodium alginate membrane with phosphoric acid for separating ethanol aqueous solution. Phosphoric acid established a linkage with sodium alginate through ester formation, as confirmed by FTIR [55].

Table 2-1. Previous investigation results of alginate membrane (1).

Authors	Year	Base cain	Concentration of base chain	Cross-linker	Concentration of cross-linker	Investigation	Tested material	Comments	Rf.
Hubble, J. et al.	1985	Sodium alginate	2-4% w/v	Calcium chloride Barium chloride	0.05M 0.05M	Ultrafiltration	Bovine serum albumin Concanavalin A Ferritin	Membrane was supported by glass fibre filter.	49
Andreopoulos, A. G. et al.	1987	Sodium alginate	1.8% w/w	Calcium sulphate dihydrate	Unknown	Vapour sorption	Methyl methacrylate	-	50
Julian, T. N. et al.	1988	Sodium alginate	3% w/w	Calcium acetate	0.1-1.0M	Permeability	Acetaminophen	-	23
Teixeira, J. A. et al.	1994	Sodium alginate	3% w/v	Calcium chloride	2% w/v	Diffusion coefficient CO_2 evolution	Glucose Malic acid	Yeast cell was immobilized in the membrane.	46
Aslani, P. and R. A. Kennedy	1996	Sodium alginate	3% w/w	Calcium acetate Zinc acetate	0.1-0.7M 0.1-0.7M	Diffusion coefficient	Acetaminohen	Drug diffusion	51
Yeom, C. K., and Lee, K.-H.	1998	Sodium alginate	2.5% w/w	Glutaraldehyde	0-20% v/v	Pervaporation	Ethanol	-	54
Zhang, W. et al.	1999	Sodium alginate	2 % w/v	Calcium chloride	2% w/v	Diffusion coefficient	Glucose Lactic acid	*Lactobacillus rhamnosus* was immobilized.	47
Yang, G. et al.	2000	Sodium alginate blend with Cellulose	0 - 8% w/w 8 - 0% w/w	Calcium Chloride	5% w/w	Pervaporation	Ethanol	-	56
Wang, X. P.	2000	Sodium alginate coated on Polyacrylonitrile	1% Commercial membrane	1,6-Hexanediamine or Poly(vinyl alcohol)	0.25% 1%	Pervaporation	Acetic acid	-	59
Grassi, M. et al.	2001	Sodium alginate	Unknown	Calcium chloride	0.05 M	Diffusion coefficient	Theophylline	Drug diffusion	41
Toti, U. S. et al.	2004	Sodium alginate	5% w/v	Glutaraldehyde	1% v/v	Pervaporation	Acetic acid Isopropanol	Different viscosity grade sodium alginatew were tested.	53
Kanti, P. et al.	2004	Sodium alginate blend with Chitosan	3% w/w 3% w/w	Glutaraldehyde	5% v/v	Pervaporation	Ethanol	-	60

http://dx.doi.org/10.5772/50734

Table 2-2. Previous investigation results of alginate membrane (2).

Authors	Year	Base Cain	Concentration of base chain	Cross-linker	Concentration of cross-linker	Investigation	Tested material	Comments	Rf.
Rhim, J.-W.	2004	Sodium alginate	2% w/v	Calcium chloride	0.04 - 0.12 g / 4g alginate 10 - 50 w/v	Physical and Mehanical properties	-	Two different methods of cross-linking were tested.	69
Smitha, B. et al.	2005	Sodium alginate blended with Chitosan	3% w/w 3% w/w	none	-	Direct methanol fuel cell	Methanol	Cross-link was used only polyion comples.	62
Zimmermann, H. et al.	2007	Sodium alginate	0.7% w/v	Barium chloride	20mM	Physical and Biological properties		NMR, CLSM, AFM, Burst pressure, Water flow	52
Kalyani, S. et al.	2008	Sodium alginate	3% w/w	Phosphoric acid	3.5 vol.%	Pervaporation	Ethanol	-	55
Reddy, A. S. et al.	2008	Sodium alginate blend with Chitosan	2% w/w 2% w/w	Calcium chloride and Maleic anhydride	2% 3.5 % w/w	Pervaporation	1,4-Dioxane	-	61
Kashima, K. et al.	2010	Sodium alginate	10g/L	Calcium chloride	0.05-1.0M	Molecular size Mechanical property Water permeability	Urea Glucose Methyl Orange Indigo Carmine Bordeaux S	Superior molecular size screening ability was found.	63
Saraswathi, M. et al.	2011	Sodium alginate blend with dextrin	20-0% w/v 0-20% w/v	Glutaraldehyde	Unknown	Pervaporation	Isopropanol	-	58
Chen, J. H., et al.	2012	Sodium alginate Hydroxyl ethyl cellulose	2.2% w/w 0.19% w/w	Glutaraldehyde	0.5% w/w	Adsorption	Cd (II) ion	-	57
Papageorgiou, S. K., et al.	2012	Sodium alginate	10.7% w/w	Calcium chloride	10%	Photocatalytic UF	Methyl orange	Alginate fiber stabilized TiO_2	14

http://dx.doi.org/10.5772/50734

3.1.2. Hybrid membrane with other polymers

Many efforts have been made to increase the performance of the alginate membrane by blending it with different hydrophilic polymers. Alginate-cellulose using a calcium ion cross-link was investigated in the permeation flux of ethanol aqueous solution for pervaporation [56]. A novel porous composite membrane was prepared using sodium alginate and hydroxyl ethyl cellulose hybrid as an immobilization matrix for humic acid, then cross-linked by glutaraldehyde [57]. Hybrid membranes of sodium alginate and dextrin were prepared by casting followed by cross-linking with glutaraldehyde and used for pervaporation separation of isopropanol aqueous solution [58]. Casting an aqueous solution of alginate with 1,6-hexanediamine or poly (vinyl alcohol) on a hydrolyzed microporous polyacrylonitrile membrane was characterized by pervaporation separation of acetic acid aqueous solution [59].

The most employed alginate hybrid material was chitosan. Polymer complex membranes made by blending 84% deacetylated chitosan and sodium alginate followed by cross-linking with glutaraldehyde were tested for separating ethanol from ethanol aqueous solution [60]. Sodium alginate and chitosan hybrid membranes were cross-linked with maleic anhydride for separating 1,4-dioxane aqueous solution. Such a membrane has good potential for breaking the aqueous azeotrope 1,4-dioxane [61].

An alginate-chitosan membrane without a cross-linker could be prepared practically. The structural formation of a chitosan-alginate ion complex was attained between the anion group ($-COO^-$) of sodium alginate and the protonated cation group ($-NH_3C$) of chitosan [62].

3.2. Preparation of a Flat Alginate Membrane

Our original procedure to prepare calcium alginate membrane by casting was as follows. One gram sodium alginate was dissolved in 100mL water. Sodium alginate samples were provided by Wako Pure Chemical Industries, Ltd. (Osaka, Japan) and KIMICA Corporation (Tokyo, Japan). Calcium chloride (0.05M to 1.0M) was also dissolved in water. Twenty grams of the sodium alginate solution was dispensed on a Petri dish and then completely dried in desiccators at room temperature (298K) for one week. A dried thin film of sodium alginate appeared on the Petri dish. Next, calcium chloride aqueous solution was added directly to the dried thin film of sodium alginate in the Petri dish. A calcium alginate membrane quickly formed in the Petri dish at room temperature. After 20min, the swollen membrane was separated from the Petri dish and then left in the dish for an additional 20min. The membrane was immersed for a total of 40min in the calcium chloride aqueous solution. The formed calcium alginate membrane was soaked in pure water to remove excess calcium chloride aqueous solution, then stored in pure water [63].

The fundamental gelling mechanism of alginate polymer was the ionic binding reaction between G-G blocks and divalent cations, such as Ca^{2+}. Alginate has high potential of ion exchange. Cross-linking quickly started in the alginate solution. A calcium alginate gel particle was easily obtained by injecting the sodium alginate solution into the calcium aqueous solution [64]. In contrast, the quickly gelling reaction inhibited the preparation of a flat alginate membrane. To overcome rapid gelling, sodium alginate aqueous solution was first dried,

and then the cross-linker aqueous solution was directly introduced into the dried alginate surface. As a result, a calcium alginate membrane having a flat surface was successfully prepared. The advanced feature of flat alginate membrane preparation was originally examined by Kashima et al. [63].

3.3. Evaluation of Components in the Alginate Polymer Chain

As mentioned in chapter 2, components in the alginate polymer chain important factors in investigating the properties of the alginate gel membrane. Two uronic acids, β-D-mannuronic acid (M) and α-L-guluronic acid (G), were constituents of the alginate molecular chain. The homopolymeric blocks of α-L-guluronic (G-G block) in the alginate chain are constructed mainly of a cross-linked zone. Hence, G-G blocks perform a dominant role in the mechanical strength and the mass-transfer characteristics of the calcium alginate membrane [65].

3.3.1. Qualitative analysis of uronic acid

Mannuronic acid lactone was used as the standard component of uronic acid. As the standard solution, various concentrations of mannuronic acid lactone were dissolved in water. The concentrations were determined by Bitter-Muir's carbazole sulfuric acid method [66], and the concentration of the colored solution was measured by optical density at 530nm. The analysis produced good intensity and accuracy of coloration [67].

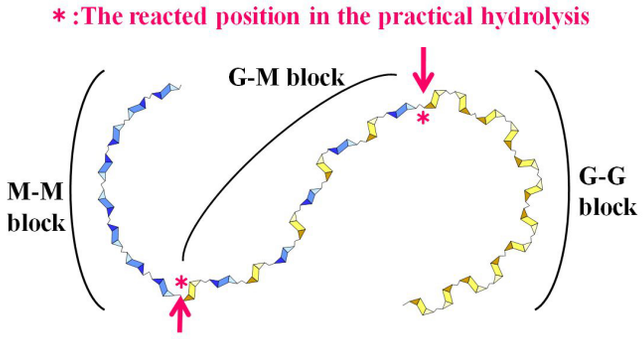

Figure 3. Sodium alginate molecular chain. The hydrolyzed site is indicated by an asterisk (*). Sodium alginate was then separated into three molecular chain blocks: M-G, M-M, and G-G.

3.3.2. Partial hydrolysis of the alginate molecular chain to determine the mass fraction of homopolymeric blocks

The mass of uronic acid in the actual alginate chain was determined by partial hydrolysis combined with Bitter-Muir's carbazole sulfuric acid method. Partial hydrolysis protocols were employed according to a previous method [67]. Figure 3 illustrates the alginate molecular chain and homopolymeric blocks. The reacted position of partial hydrolysis is marked by an asterisk (*). The sodium alginate chain was separated into three molecular chain blocks (M-G, M-M, and G-G).

Sodium alginate (0.5g) was dissolved in 0.3M HCl (50mL). The resulting solution was heated in an electrical blast-drying chest (373K) for 2h to promote partial hydrolysis. The partial hydrolysis solution was then centrifuged (3000min^{-1}, 15min), and a sample solution of the M-G block was obtained as the supernatant.

The precipitate was mixed with pure water (10mL), and 3M NaOH was added to aid dissolution. The concentration was then adjusted to 1% by the addition of pure water, and NaCl was introduced to achieve 0.1M of sodium alginate. The solution was adjusted to pH 2.9 using 2.5M HCl and then centrifuged (3000min^{-1}, 15min). The sample solution of the M-M block was obtained as the supernatant.

After filtration, the precipitate was mixed with pure water (10mL) and dissolved by adding 3M NaOH, yielding the sample solution of the G-G block. As a result, three sample solutions (M-G, M-M, and G-G) were obtained.

3.3.3. Mass fraction of homopolymeric blocks of α-L-gluronic acid

The mass of the M-G block in the sodium alginate (W_{MG}) was directly obtained from the concentration of the M-G block sample. The mass of the M-M block (W_{MM}) and that of the G-G block (W_{GG}) in the sodium alginate were also obtained independently in the same manner. The mass fraction of α-L-guluronic acid in the sodium alginate (F_G) was then calculated using the following formula:

$$F_G = \frac{W_{GG} + W_{MG} \times P}{W_{GG} + W_{MG} + W_{MM}} \quad (1)$$

where P is the partial mass fraction of α-L-guluronic acid in the M-G block. The polymeric structure of the calcium alginate gels was constructed mainly by intermolecular ionic bonds in the homopolymeric blocks of the α-L-guluronic acid junction zone, in combination with Ca^{2+} [42]. Therefore, in our study, P is assumed to be negligible (P = 0), and Eq. (1) is rearranged as follows.

$$F_{GG} = \frac{W_{GG}}{W_{GG} + W_{MG} + W_{MM}} \quad (2)$$

The mass fraction of the homopolymeric blocks of α-L-guluronic acid (F_{GG}) was therefore obtained from natural resources. It was considered a key factor in regulating membrane properties.

3.4. Morphology of the Calcium Alginate Membrane

No stable calcium alginate membrane was obtained using a very low concentration (e.g. less than 0.01M) of $CaCl_2$. It looked like jelly (Figure 4a). A stable, flat, thin membrane was obtained with more than 0.05M $CaCl_2$ solution as a cross-linker (Figure 4b). The membrane became transparent with increasing $CaCl_2$ concentration (Figures 4c, d).

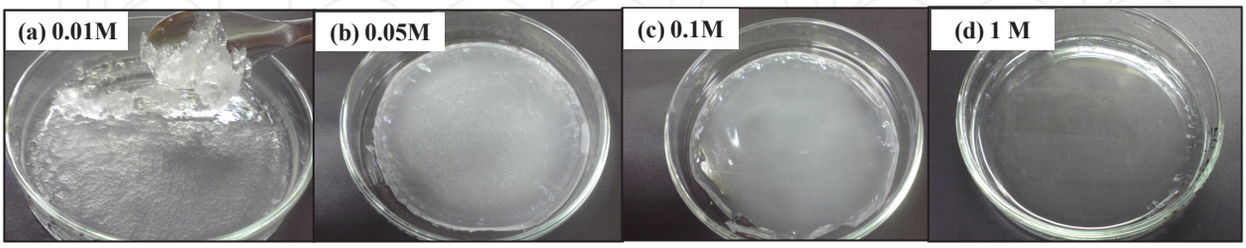

Figure 4. Pictures of calcium alginate membrane. (a) $CaCl_2$: 0.01M, (b) $CaCl_2$: 0.05M, (c) $CaCl_2$: 0.1M, (d) $CaCl_2$: 1M.

In scanning electron microscopy (SEM) (Miniscope TM-1000, Hitachi, Ltd., Tokyo, Japan), the surface of the membrane appeared to be smooth. No pores were observed on the surface. The higher F_{GG} membrane had a dense surface (Figure 5a), whereas the lower F_{GG} membrane appeared harsh (Figure 5b). Regardless of F_{GG}, the membrane surface observed by SEM became smoother with increasing $CaCl_2$ concentration (Figures 5a, b, c, d).

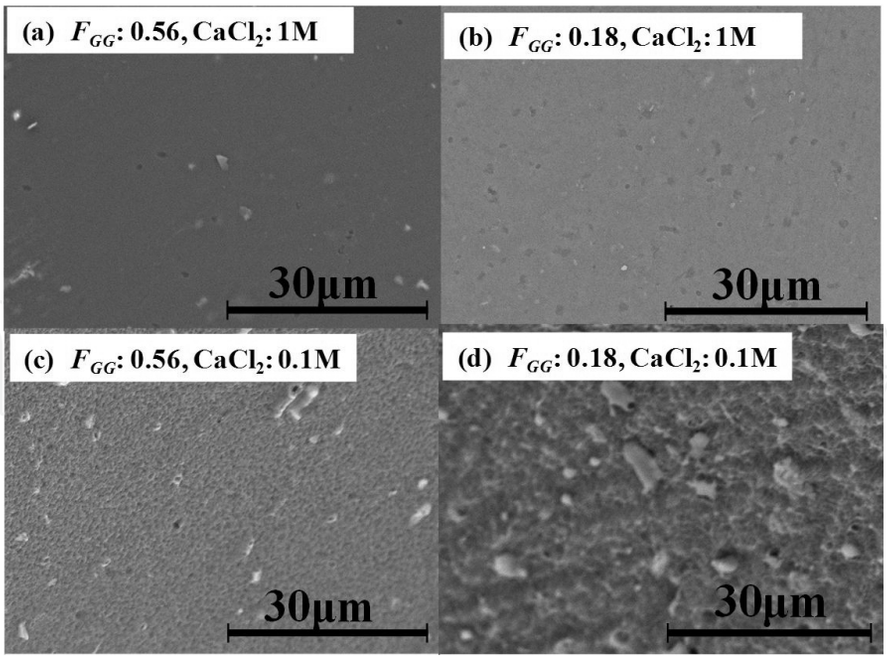

Figure 5. Scanning electron microscopy (SEM) images of the surface of the calcium alginate membrane. (a) F_{GG}: 0.56, $CaCl_2$: 1M. (b) F_{GG}: 0.18, $CaCl_2$: 1M. (c) F_{GG}: 0.56, $CaCl_2$: 0.1M. (d) F_{GG}: 0.18, $CaCl_2$: 0.1M.

http://dx.doi.org/10.5772/50734

Figure 6 presents scanning probe microscope (SPM) (S-image SII Nano Technology, Inc., Tokyo, Japan) images of the membrane surfaces. SPM can determine the morphology of the membrane surface by using the physical force (e.g., atomic force) between the cantilever and the sample membrane. In our case, dynamic force mode/microscopy (DFM) was used for observation. DFM is a measurement technique based on making the cantilever resonant to detect gravitation and repulsive forces against the sample surface. It is a morphology measurement mode for stable observation of relatively sticky, uneven, and soft samples (e.g., biopolymers). The distribution of membrane asperity clearly decayed with increasing F_{GG} (Figures 6a, b). In contrast, with a low concentration of calcium, the distribution of membrane asperity changed little (Figures 6c, d). These results suggest that the molecular framework was condensed by increasing F_{GG}. With higher $CaCl_2$ concentration (1.0M), the effect of F_{GG} became dominant and made a smooth surface. However, with lower $CaCl_2$ concentration (0.1M), the effect of F_{GG} was insignificant, and the membrane surface did not become smooth.

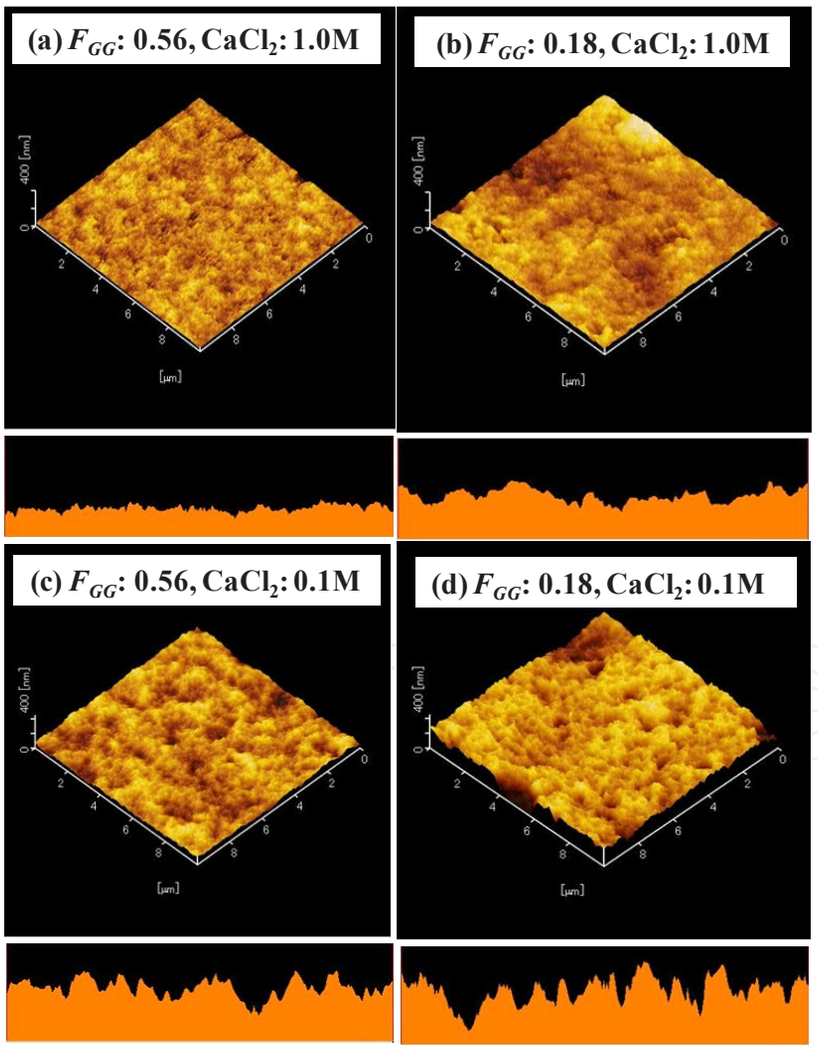

Figure 6. Scanning probe microscopy (SPM) views of the surface of the calcium alginate membrane. (a) F_{GG}: 0.56, $CaCl_2$: 1M. (b) F_{GG}: 0.18, $CaCl_2$: 1M. (c) F_{GG}: 0.56, $CaCl_2$: 0.1M. (d) F_{GG}: 0.18, $CaCl_2$: 0.1M.

4. Mechanical Properties of the Calcium Alginate Membrane

Investigation of mechanical properties is important for practical application. The following section describes the maximum stress and strain at membrane rupture of the calcium alginate membrane involved with calcium concentration and F_{GG}.

4.1. Investigation of Mechanical Strength

The maximum stress and strain at membrane rupture is evaluated by rheometer as a general test of the mechanical properties of the polymer membrane. A swollen membrane sample (10mm wide and 30mm long) was mounted in the rheometer (CR-DX500, Sun Scientific Co., Ltd., Tokyo, Japan) with a crosshead speed of 2mm/s. Maximum stress [N/m^2] at membrane rupture was evaluated based on the loading force divided by the cross-sectional area of the membrane. Maximum strain was evaluated as the percentage by which the length increased at membrane rupture divided by the original length of the membrane sample. The relationship between maximum stress and strain with deacetylation degree was investigated as an elastic property of the chitosan membrane using this method [4].

4.2. Effect of Calcium Concentration

Figure 7 depicts the effect of $CaCl_2$ concentration on the maximum stress at membrane rupture. The maximum stress increased with increasing $CaCl_2$ concentration as a cross-linker. With higher F_{GG} (F_{GG} = 0.56), the maximum stress increased remarkably, especially with higher $CaCl_2$ concentration.

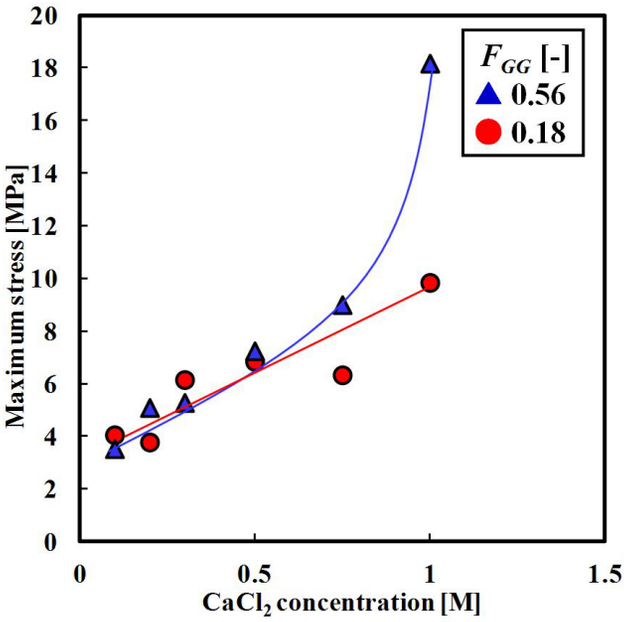

Figure 7. Effect of $CaCl_2$ concentration on maximum stress at membrane rupture.

http://dx.doi.org/10.5772/50734

In contrast, the maximum strain at membrane rupture was remarkably reduced by adding $CaCl_2$ (Figure 8). The cross-linked site became more highly populated with increasing $CaCl_2$ concentration. It was resulted increasing the mechanical strength [63]. Using $CaCO_3$ as a cross-linker, the mechanical properties exhibited profiles similar to those using $CaCl_2$ [68].

4.3. Effect of Mass Fraction of the Homopolymeric Blocks of α-L-Guluronic Acid (F_{GG})

Mechanical strength and elastic characteristics apparently changed with F_{GG}. Maximum stress increased remarkably with increasing F_{GG} at the same Ca^{2+} concentration (Figure 7). In contrast, when the membrane ruptured, maximum strain was remarkably reduced with increasing F_{GG} (Figure 8). Increasing F_{GG} obviously enhanced the polymeric framework of the membrane.

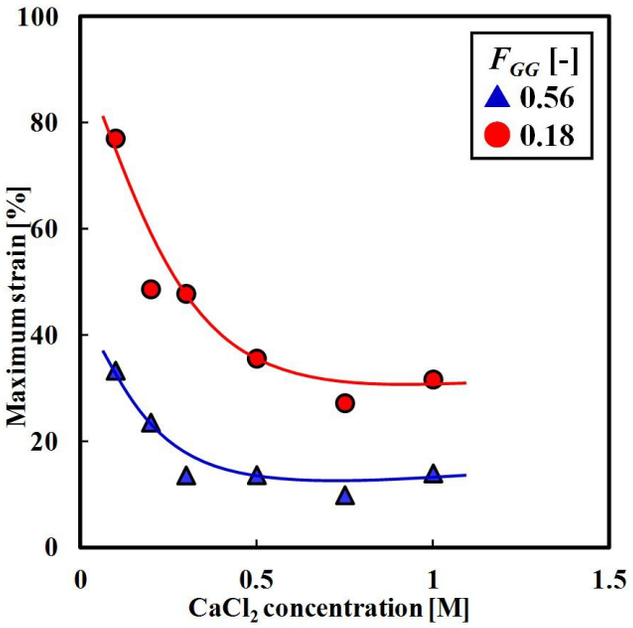

Figure 8. Effect of $CaCl_2$ concentration on maximum strain at membrane rupture.

4.4. Effect of Cross-Linking Methods

The mechanical properties of calcium alginate membranes prepared from two different $CaCl_2$ treatments were examined by Rhim [69]. One is the direct mixing of $CaCl_2$ into a membrane-making solution (mixing membrane). The other is the immersion of alginate membrane into $CaCl_2$ solution (immersion membrane). With the mixing method, maximum stress and maximum strain at the break of the mixing membrane did not change with increased addition of $CaCl_2$. In contrast, for the immersion membrane, the maximum stress increased and the maximum strain decreased with increased addition of $CaCl_2$. The membrane became rigid. In the immersion method, the mechanical characteristics were strongly influenced by $CaCl_2$ concentration.

4.5. Effect of Relative Humidity

The effect of relative humidity on the mechanical properties of the calcium alginate membrane was examined at relative humidities of 59%, 76%, 85% and 98% at room temperature for 8 days [70]. As relative humidity increased, maximum strain increased and maximum strength decreased.

4.6. Comparison with Other Membranes

Figure 9 indicates the mechanical properties of various polymer membranes. The calcium alginate membrane exhibited high stress and low strain at rupture. It had better mechanical properties than other biopolymer membranes (e.g., chitosan [4] and cellulose acetate [71]). The higher F_{GG} membrane had higher mechanical strength at rupture, with elasticity. However, the lower F_{GG} membrane was flexible and had desirable mechanical strength.

For comparison, the polytetrafluoroethylene (PTFE)/polyvinyl alcohol (PVA) composite membrane had stronger mechanical strength and very low maximum strain, with rigidity [72] (Figure 9).

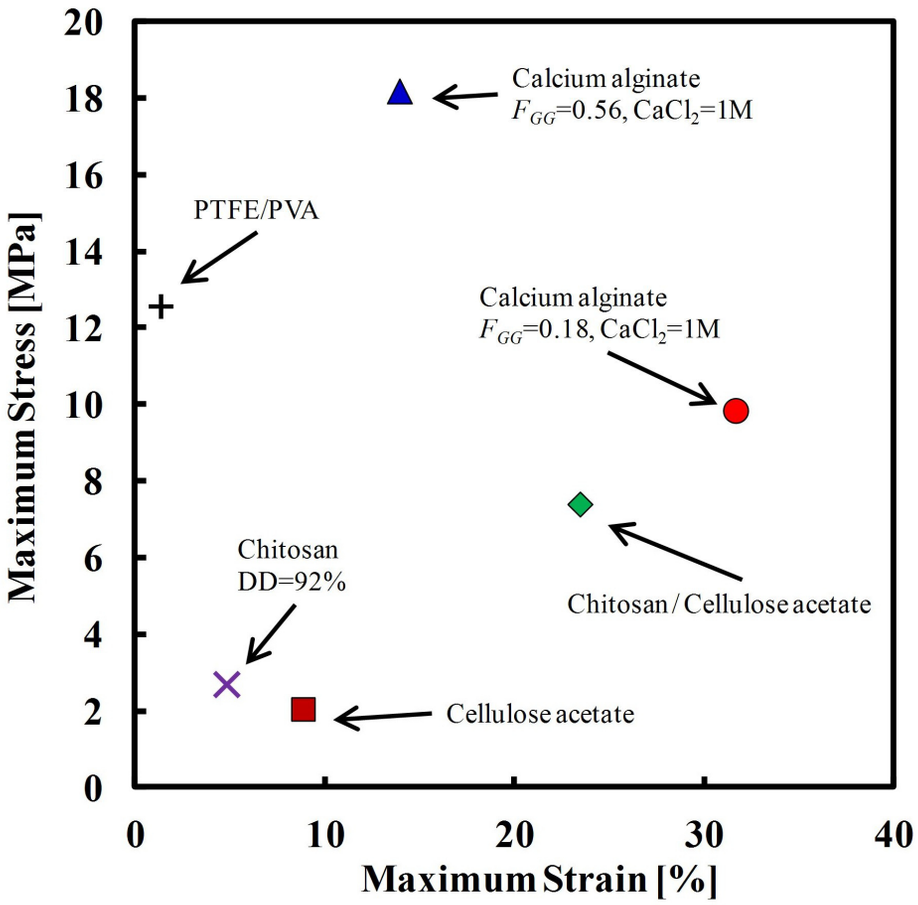

Figure 9. Mechanical strength of alginate membrane compared with various polymer membranes.

http://dx.doi.org/10.5772/50734

5. Water Content in a Swollen Membrane

The water content of a hydrophilic membrane influences the diffusion phenomena and water permeability. In general, polymer membranes having higher water content have higher water permeability, that has been reported in cellulose acetate membranes [73]. As water occupied mainly the void of the membrane, volumetric water content is often regarded as the void fraction of the membrane structure [74].

5.1. Evaluation of Water Content

The volumetric water content of the swollen membrane was not measured directly. Instead, it was evaluated from the mass-based water content (H_M) using gravimetric methods. The swollen membrane is assumed to have equilibrium water content. Excess water attached to the membrane surface was removed using filter paper. The mass of the swollen sample (w_e) was measured initially, then, after drying (333K for 24h), the mass of the dried membrane at equilibrium state (w_d) was measured. For strict analysis, w_d included "bonding water" on polymer networks. It is assumed to be negligible in the following description [45].

The difference between w_e and w_d represents the mass of the total contained water (w_t).

$$w_t = w_e - w_d \tag{3}$$

The mass-based water content of the swollen membrane (H_M) was then calculated using the following equation.

$$H_M = \frac{w_e - w_d}{w_e} = \frac{w_t}{w_e} \tag{4}$$

The volume of water contained in the membrane void was evaluated from w_t/ρ_W. The apparent volume of the swollen membrane was estimated as w_e/ρ_M. The apparent density of the swollen membrane ρ_M was determined from the mass of the swollen membrane w_e divided by the apparent volume of the swollen membrane, which was calculated from the membrane area (square with 4cm sides) and its thickness. The estimated volumetric water fraction of the swollen membrane (H_V) was calculated using Eq. (5).

$$H_V = \frac{(w_t / \rho_W)}{(w_e / \rho_M)} \tag{5}$$

H_V is often employed as the void fraction (porocity) of the swollen-state membrane. The volumetric water content (H_V) in the calcium alginate membrane is presented in Figure 10. H_V gradually decreased with increasing $CaCl_2$ concentration.

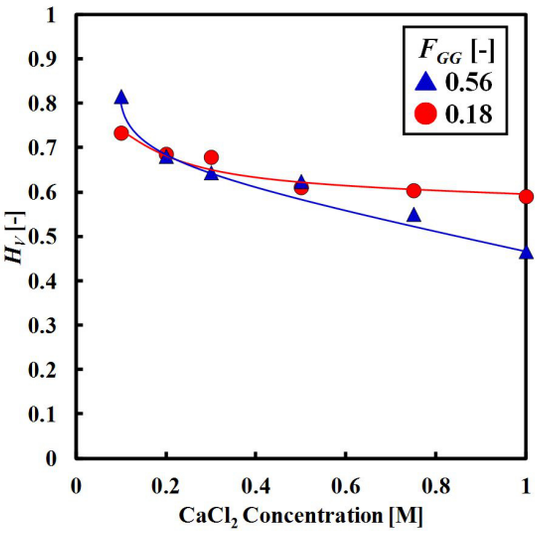

Figure 10. Effect of $CaCl_2$ concentration on volumetric water content H_V.

5.2. Effect of Calcium Ion and F_{GG} on Water Content in Membrane

The dry-based water content of calcium alginate gel beads loading sucrose has been investigated for encapsulation-dehydration of plant germplasm [75]. The dry weight of the beads decreased, and the water content increased with increasing cross-linking time (10 to 30min). The sucrose was diffused to the outer aqueous phase, and then the water penetrated into the gel beads. This is understood as osmotic phenomena surrounding the gel particles. The mass fraction of unfrozen water compared to total water content was also investigated as the thermal property of the gel beads. It increased within 5 to 15min to achieve maximum level (23%), and then declined to minimum level (17%) at 30min.

The H_V of the swollen membrane gradually decreased with increasing F_{GG} [65]. The effect of F_{GG} was especially strong with higher $CaCl_2$ concentration (Figure 10). The lower F_{GG} membrane had higher water content, in spite of the high $CaCl_2$ concentration. The cross-linking molecular chain decreased with lower F_{GG}.

5.3. Stability of the Swollen Membrane

The stability of the swollen membrane is important to long-life use in practical applications. Rhim focused on the gravimetrical change of the membrane before and after practical use. Stability was evaluated by the dry-base mass of the membrane [69]. Rhim focused on the gravimetrical change of the membrane before and after practical use. Stability was evaluated by the dry-base mass of the membrane [69]. The membrane mass decreased 16% to 20% with increasing soaking temperature (298K to 353K) in aqueous phase. This change was induced by dissolving the membrane matter into aqueous phase. In contrast, the change in membrane mass did not present any significant difference with $CaCl_2$ concentration. The stability of the membrane was affected by soaking temperature but did not depend on $CaCl_2$ concentration.

http://dx.doi.org/10.5772/50734

5.4. Void Fraction of Membrane

The water content of a membrane can be regarded as an indicator of the void fraction (ε) of the membrane structure [74]. Al-Rub et al. found that membrane distillation mass flux increased linearly with the membrane void fraction, whereas the temperature difference increased slightly with an increase in membrane void fraction [76]. This is due to the fact that a higher void fraction means that more mass-transfer channels exist for diffusion; hence, higher flux results. The void fraction of commercial microfiltration membranes varies from 60% to 90%, depending on material type, membrane form (flat sheet or hollow fiber), and manufacturing method [77]. The calcium alginate membrane has a high void fraction (50% to 90%) [63].

6. Mass-transfer Characteristics

The diffusivity in calcium alginate "beads" has often been investigated. The effective diffusion coefficient of the alginate "membrane" was originally reported by Kashima et al. [63]. The effective diffusion coefficients are listed in Table 3 and plotted in Figure 11.

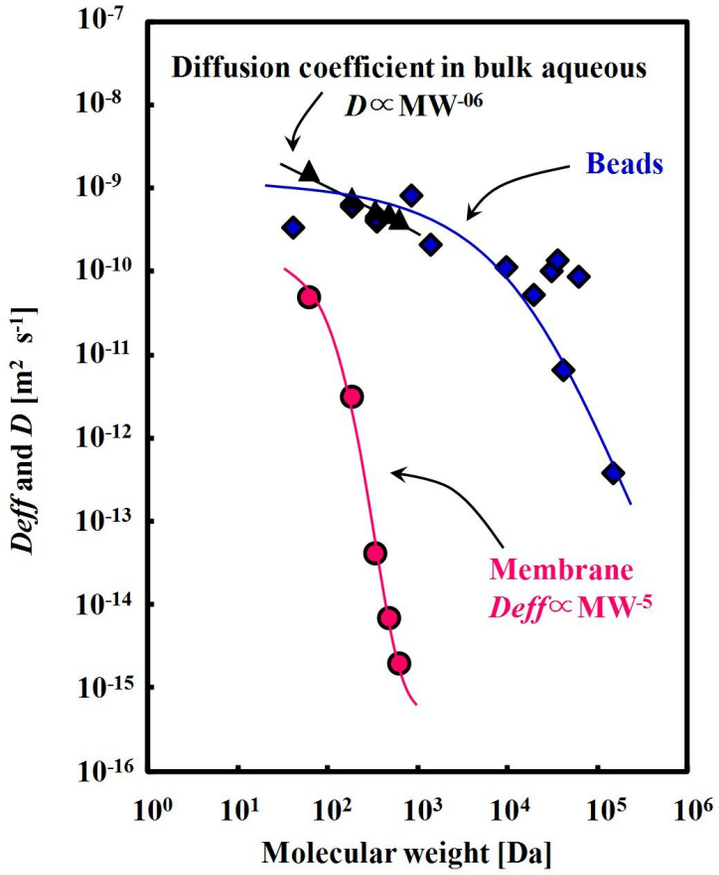

Figure 11. Effective diffusion coefficient of calcium alginate gel.

Table 3. Effective diffusion coefficient in calcium alginate gels.

Authors	Year	Base chain	Concentration of base chain	Cross-linker	Concentration of cross-linker	Gel type	Diffusion conponent	MW [Da]	Effective diffusion coefficient [$m^2 s^{-1}$]	Rf.
Mehmetoglu, U.	1990	Calcium alginate	5%	Calcium chloride	0.05M	Beads	Sucrose	342	4.10×10^{-10}	84
Longo, M. A. et al.	1992	Calcium alginate	2% w/v	Calcium chloride	3% w/v	Beads	*Bacillus* total protease	30000	1.04×10^{-10}	85
							Bacillus metalloprotease	35000	1.40×10^{-10}	
							Serratia total protease	60000	8.90×10^{-11}	
Kikuchi, A. et al.	1999	Calcium alginate	2% w/w	Calcium chloride	0.1M	Beads	Ca^{2+}	40	3.47×10^{-10}	86
							Brilliant Blue	826	8.41×10^{-10}	
							Dextran	9400	1.16×10^{-10}	
								19000	5.39×10^{-11}	
								40500	6.73×10^{-12}	
								145000	3.90×10^{-13}	
Dembczynski, R. and T. Jankowski	2000	Calcium alginate	1% w/v	Calcium chloride	4% w/v	Beads	Glucose	180	6.58×10^{-10}	39
							Fructose	180	6.18×10^{-10}	
							Sucrose	342	4.70×10^{-10}	
							Lactose	342	4.51×10^{-10}	
							Vitamin B12	1355	2.16×10^{-10}	
Koyama, K. and M. Seki	2004	Calcium alginate	2% w/v	Calcium chloride	1% w/v	Beads	Glucose	180	6.50×10^{-10}	87
Kashima, K. et al.	2010	Calcium alginate	1% w/v	Calcium chloride	1M	Membranes	Urea	60	5.06×10^{-11}	65
							Glucose	180	3.22×10^{-12}	
							Methyl Orange	327	4.24×10^{-14}	
							Indigo Carmine	466	7.07×10^{-15}	
							Bordeaux S	604	2.02×10^{-15}	

http://dx.doi.org/10.5772/50734

6.1. Analysis of Mass-Transfer

The typical procedure to measure mass-transfer flux is as follows. The overall mass-transfer coefficient K_{OL} was determined by measuring the mass-transfer flux based on Eqs. (6) and (7). The membrane was sandwiched between twin glass mass-transfer cells that were placed in a thermostatic bath (298K).

$$\ln\left(1-\frac{2C_s}{C_{fi}}\right)=-2\frac{A}{V}K_{OL}t \tag{6}$$

$$K_{OL}^{-1}=k_{L1}^{-1}+k_m^{-1}+k_{L2}^{-1} \tag{7}$$

Both aqueous phases were sufficiently stirred to create a fully developed turbulent flow. Film mass-transfer resistances k_{L1}^{-1} and k_{L2}^{-1} in the overall mass-transfer resistance K_{OL}^{-1} were ignored under fully turbulent conditions. In this case, K_{OL} did not depend on stirring rate. Therefore, it directly indicated the membrane mass-transfer coefficient km ($km = D_{eff}/l$). The effective diffusion coefficient in the membrane (D_{eff}) was evaluated from km. The initial thickness of the swollen membrane l was measured with a micrometer (Mitutoyo Corporation, Kawasaki, Japan). The molecular-size screening capability of the calcium alginate membrane was investigated by measuring mass-transfer flux using various molecular-size indicators (Urea 60 Da, Glucose 180 Da, Methyl orange 327 Da, Indigo carmin 466 Da, and Bordeaux S 604 Da) [63].

The concentration of the stripping solution was determined by a spectrophotometer (UV Mini 1240, Shimadzu, Kyoto, Japan). The absorbances of the color pigments employed (Methyl orange, Indigo carmine, and Bordeaux S) were measured based on the maximum wavelength (Methyl orange 462nm, Indigo carmine 610nm, and Bordeaux S 520nm). The concentration of urea was determined by absorbance 570nm, according to the urease-indophenol method (Urea NB, Wako Pure Chemical Industries, Ltd., Osaka, Japan). The concentration of glucose was determined by absorbance 505nm, according to the mutarotase-GOD method (Glucose C2, Wako Pure Chemical Industries, Ltd., Osaka, Japan).

6.2. Molecular-Size Screening

Remarkable size-screening capability was obtained between 60Da (Urea) and 604Da (Bordeaux S). The effective diffusion coefficient in the membrane D_{eff} decreased 2.5×10^4-fold even though the molecular-size increased only 10-fold [63] (Figure 11). This result strongly suggests that the mass-transfer channel was mono-disperse for molecular-sizes in our experiment. Wu and Imai reported that large dependence on molecular-size was achieved by specific polymer frameworks using pullulan and κ-carrageenan composite membranes [78].

The remarkable size-screening capability presented in Figure 11 was achieved by prepared 1.0M $CaCl_2$. The membrane composition was expressed as 0.1[mol-Ca^{2+}g-sodium alginate^{-1}], which is the molar ratio of molar Ca^{2+} to unit mass of alginate. The molar ratio of Ca^{2+} to alginate polymer is a dominant parameter of membrane preparation.

The diffusion coefficient in bulk aqueous phase D was plotted for comparison. It depended on the -0.6th power of the molecular weight. In contrast, the effective diffusion coefficient depended on almost the -5th power of the molecular weight of the tested components. The tested component did not adsorb to the membrane. The large dependence of the effective diffusion coefficient on molecular weight was due to the polymeric framework of a calcium alginate membrane, not due to adsorption. In contrast, the polymeric framework became dense to prepare the membrane (Figure 11).

6.3. Mass-Transfer Characteristics of Urea

The effective diffusion coefficient of urea (60Da) was evaluated mainly for mass-transfer characteristics as a typical small molecule.

6.3.1. Effect of Calcium Ion and F_{GG} on Mass-Transfer

The effective diffusion coefficient gradually decayed with increasing $CaCl_2$ concentration, due to the progress of cross-linking of molecular frameworks in the membrane (Figure 12). At $CaCl_2$ concentrations above 0.1M, the dependence of the effective diffusion coefficient on the $CaCl_2$ concentration became small [63]. This trend indicates that the molecular frameworks became saturated in this range, and that the effective diffusion coefficient remained almost constant. $CaCl_2$ acted as a cross-linker of molecular frameworks in the alginate molecular chain.

In the higher $CaCl_2$ concentration range, the effect of F_{GG} on the effective diffusion coefficient was especially remarkable (Figure 12). The polymeric structure of calcium alginate gels was governed mainly by intermolecular ionic bonds with homopolymeric blocks of the α-L-guluronic acid junction zone, in combination with Ca^{2+} [24].

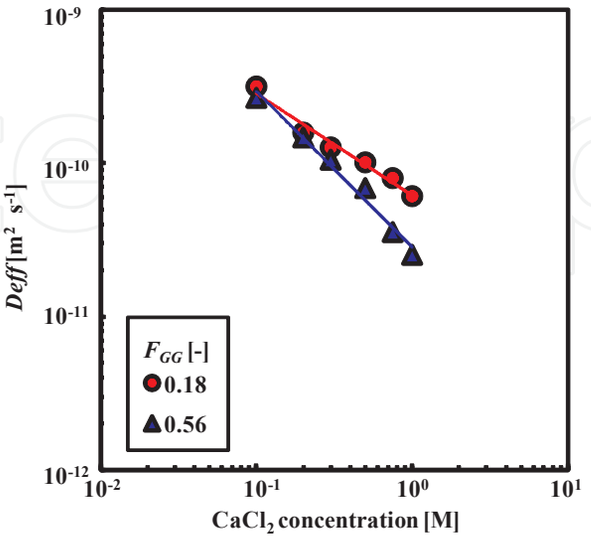

Figure 12. Effect of calcium chloride concentration on the effective diffusion coefficient of urea.

http://dx.doi.org/10.5772/50734

6.3.2. Effect of Water Content

The relationship between the effective diffusion coefficient and the volumetric water content of the membrane has been discussed using Eq. (8) by Yasuda's free volume theory [79].

$$\ln\left(\frac{D_{eff}}{D}\right) = -\frac{b(1-a)x}{1+ax} \tag{8}$$

Here, $x = (H_V^{-1}-1)$, $a = V_{fm}/V_{fl}$ and $b = V^*/V_{fl}$. H_V is the volumetric water fraction of the swollen membrane, a is the free volume ratio of the dry membrane (V_{fm}) to that of solvent (V_{fl}), and b is the volumetric ratio of the permeant characteristic volume (V^*) to the free volume in the solvent (V_{fl}). D is the diffusion coefficient in bulk solvent calculated by the Wilke-Chang equation [80]. D_{eff} is the effective diffusion coefficient in the membrane. With this theory, ln (D_{eff} / D) is not generally a linear function of (H_V^{-1}-1).

There are two special cases of Eq. (8). First, ln (D_{eff} / D) becomes independent of membrane swelling at low H_V ($x \to \infty$). The left-hand term of Eq. (8) becomes almost constant. D_{eff} has a very low value. Second, for a region of high H_V ($x \to 0$), the effective diffusion coefficient is relatively large and decreases with decreasing H_V. In this case, ln (D_{eff} / D) is linearly proportional to (H_V^{-1}-1) and presents a negative slope of $b(1 - a)$.

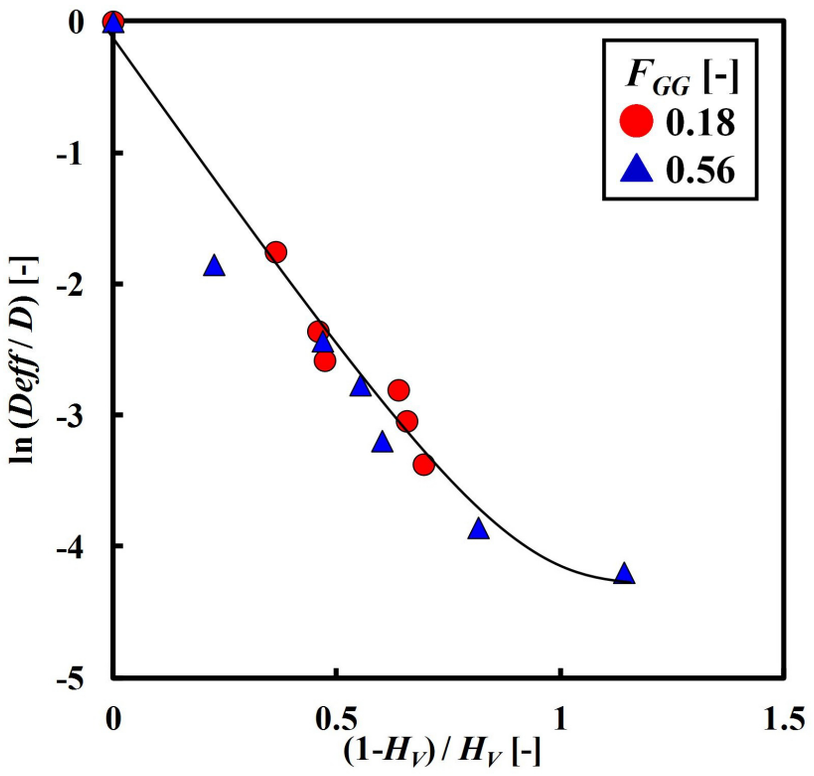

Figure 13. Effective diffusion coefficient of urea in calcium alginate membrane regulated by $CaCl_2$ concentration and F_{GG}, based on Yasuda's free volume theory.

Figure 13 depicts the ln (D_{eff} / D) of urea in a swollen calcium alginate membrane, based on the free volume theory (Eq. (8)). Here, ln (D_{eff} /D) vs. (H_V^{-1}-1) was linearly proportional with a negative slope. This trend has been reported for highly swollen membranes and/or very water-soluble solutes [81-82]. These two points were incorporated into our experiment conditions.

Ln (D_{eff} /D) vs. (H_V^{-1}-1) overlapped, regardless of having different F_{GG}. This result suggested that the value of (1 - a) and b are constant in our experiment range of F_{GG}.

(1 - a) represents the volumetric ratio of the void increased by membrane swelling due to the solvent. For urea transportation, the effect of F_{GG} on the free volume of the mass-transfer channel was not significant. In the future, the mass-transfer of other larger molecules in the membrane should be examined.

6.3.3. Tortuosity

The effective diffusion coefficient in porous materials can be represented by the following diffusion model. This model was applied to analyze mass-transfer in a swollen membrane.

$$D_{eff} = \frac{D\varepsilon}{\tau} \tag{9}$$

Here ε is the void fraction and τ is the tortuosity of the membrane. The void fraction was assumed to be the volumetric water fraction of the swollen membrane (H_V) [74].

$$\tau = \frac{DH_V}{D_{eff}} \tag{10}$$

The membrane tortuosity (τ) reflects the length of the mass-transfer channel compared to membrane thickness. Simple cylindrical mass-transfer channels across the membrane pass through at right angles to the membrane surface when tortuosity is unity (i.e., the average length of the channel is equivalent to membrane thickness). Channels usually take a more meandering path through the membrane; thus, typical tortuosities range from 1.5 to 2.5 [83].

Tortuosity of the calcium alginate membrane increased from 16 to 32 with increasing F_{GG}, which changed from 0.18 to 0.56 ($CaCl_2$ concentration of 1M). This result indicated that the mass fraction of α-L-guluronic acid was the dominant factor regulating tortuosity. However, the specific reason for a high level of tortuosity is not clear at present. Other factors inhibiting diffusion in the membrane could be speculated, (e.g., adsorption on the polymer network or molecular affinity between alginate polymer chains and the tested molecules) [65].

http://dx.doi.org/10.5772/50734

7. Water Permeation Flux

Water permeation flux is standard technical data for analyzing mass-transfer characteristics of the membrane [88]. Water permeation flux was evaluated based on the gravimetric or volumetric amount of water passing through the membrane. Gravimetric permeate flux (J_M) was generally calculated using the following equation.

$$J_M = \frac{M_P}{At} \tag{11}$$

Here, M_p is the permeate mass [kg], A is the membrane area [m^2], and t is the permeate time [s] [89]. Volumetric permeate flux (J_V) was calculated according to the following equation [90].

$$J_V = \frac{V_P}{At} \tag{12}$$

Here, V_P is the permeated volume of water (m^3), obtained from M_P / ρ_w. Wu and Imai investigated the water permeation flux of the pullulan-κ-carrageenan composite membrane [78].

7.1. Water Permeation Experiment

The typical procedure to measure water permeation flux is as follows. The permeation flux of the calcium alginate membrane was determined from the water mass flux using an ultrafiltration apparatus (UHP-62K, Advantec, Tokyo, Japan). The initial volume of feed solution was constant at 200ml. The operational pressure was adjusted by introducing nitrogen gas. The mass of permeated water was accurately measured by an electric balance and converted to volumetric water flux by recalculation using the density of the permeated water [63]. The experiment was carried out at 298K.

7.2. Effect of Cross-Linker Concentration on Water Permeation Flux

The water permeation flux decreased remarkably with increasing calcium chloride concentration due to progressive cross-linking of the molecular frameworks [63]. High water permeation flux was achieved with low $CaCl_2$ concentration as a cross-linker.

7.3. Dependence on Operational Pressure

Figure 14 illustrates the relationship between volumetric water flux and operational pressure ΔP on the calcium alginate membrane prepared by 1M $CaCl_2$. The water permeation flux increased almost linearly with increasing operational pressure. The water permeation mechanism was assumed to be Hagen-Poiseuille flow. High water permeation flux was realized in the low F_{GG} (0.18) membrane.

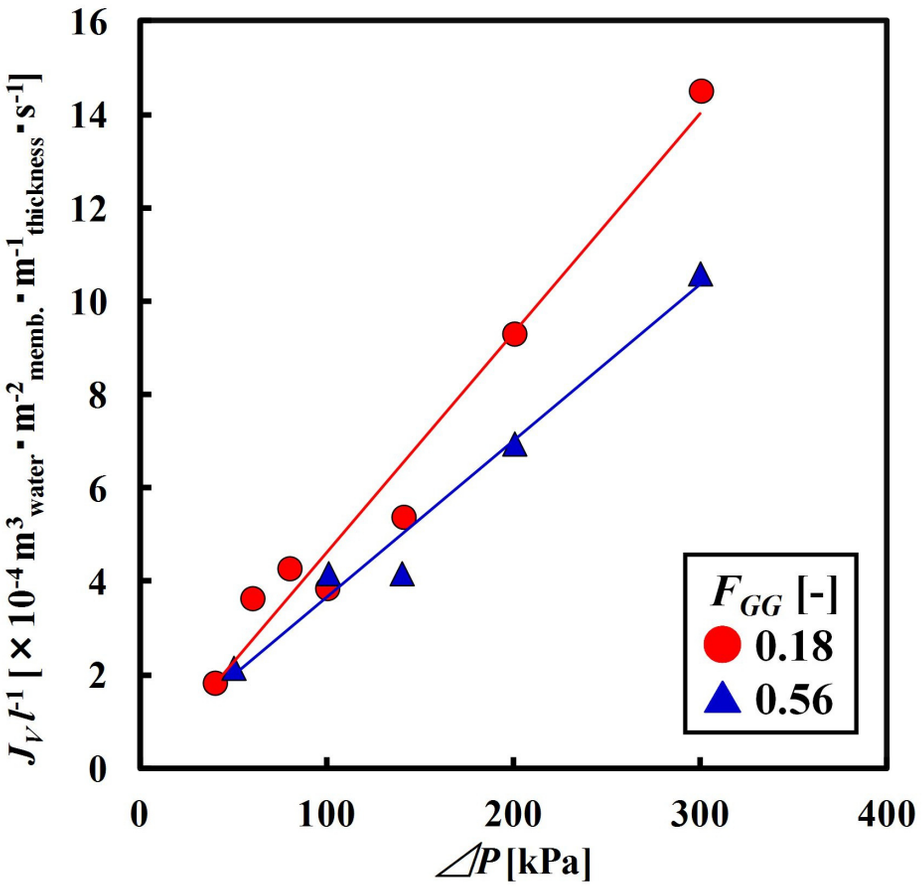

Figure 14. Water permeation flux of calcium alginate membrane ($CaCl_2$: 1M) prepared from different F_{GG} by applying different pressures.

7.4. Water Permeation Flux of Other Membranes

Table 4 presents previous investigation results of the water permeation flux of various membranes. The pure water flux of the calcium alginate membrane at ⊿ *P* 20 [kPa] was obtained as 9.3 ×10^{-9} [m^3 m^{-2} s^{-1}], which is lower than that of chitosan [45], cellulose acetate [91], and cellulose acetate with polyethylene glycol (PEG) [91]. It was assumed that the polymer framework of the calcium alginate membrane became remarkably dense, which led to decreasing water permeation flux.

Ethanol aqueous solution was previously examined in pervaporation using a sodium alginate membrane cross-linked by phosphoric acid. The permeation flux (1.3×10^{-5} kg m^{-2} s^{-1}) was less than that of the PTMSP (poly (1-trimethylsilyl-1-propyne)) membrane (5.8×10^{-5} kg m^{-2} s^{-1}) [55, 92]. The sodium alginate membrane blended with dextrin was cross-linked with glutaraldehyde to make a stable membrane. It exhibited better water permeation flux of isopropanol aqueous solution than the PVA coating alginate membrane [58, 93]. The water permeation flux was improved with the use of the PVA single component membrane presented by Naidu et al. [94].

Authers	Membrane	Driving mechanism	Permeated solution	Water concentration	P [kPa]	J_M [kg m^{-2} s^{-1}]	J_V [m^3 m^{-2} s^{-1}]	Rf.
Kashima et al.	Calcium alginate	Pressure	Pure water	-	20	-	9.3×10^{-9}	63
Takahashi et al.	Chitosan	Pressure	Pure water	-	20	-	3.4×10^{-8}	45
Saljoughi et al.	Cellulose acetate	Pressure	Pure water	-	20	-	2.2×10^{-6}	91
	Cellulose acetate - PEG		Pure water	-	20	-	6.1×10^{-5}	
Kalyani et al.	Sodium alginate	Pervaporation	Ethanol + Water	9.74 wt.%	6.7×10^{-3}	1.3×10^{-5}	-	55
Claes et al.	PTMSP	Pervaporation	Ethanol + Water	10 wt.%	4×10^{-3}	5.8×10^{-5}	-	92
	PTMSP - silica		Ethanol + Water	10 wt.%	4×10^{-3}	1.6×10^{-4}	-	
Saraswahi et al.	Sodium alginate	Pervaporation	Isopropanol + Water	10 wt.%	1.33	1.9×10^{-5}	-	58
	Sodium alginate-Dextrin		Isopropanol + Water	10 wt.%	1.33	3.7×10^{-5}	-	
Kurkuri et al.	Sodium alginate - PVA (75:25)	Pervaporation	Isopropanol + Water	10 wt.%	1.33	6.7×10^{-6}	-	93
	Sodium alginate - PVA (50:50)		Isopropanol + Water	10 wt.%	1.33	9.4×10^{-6}	-	
	Sodium alginate - PVA (25:75)		Isopropanol + Water	10 wt.%	1.33	1.1×10^{-5}	-	
Naidu et al.	PVA	Pervaporation	Isopropanol + Water	10 wt.%	1.33	2.6×10^{-5}	-	94
	PVA - Polyaniline		Isopropanol + Water	10 wt.%	1.33	1.9×10^{-5}	-	

PEG: polyethylene glycol, PTMSP: Poly (1-trimethylsilyl-1-propyne), PVA: Polyvinyl alcohol

Table 4. Water permeation flux of pressure-derived permeation (J_V) and pervaporation (J_M).

8. Conclusion

Advanced membrane material from marine biological polymer and sensitive molecular-size recognition for promising separation technology were demonstrated. Stable calcium alginate membrane in swollen state was successfully prepared. The calcium alginate membrane has better mechanical properties than other biopolymer membranes for conventional use. The calcium alginate membrane has a high void fraction (50% to 90%) similar to commercial microfiltration membrane (60% to 90%). Mass transfer characteristics are evidently changed by the mass fraction of α-L-guluronic acid (F_{GG}) and additive $CaCl_2$. Water permeation flux of the calcium alginate membrane is lower than that of other biopolymer membrane (e.g. chitosan, cellulose). In future, the water permeation flux is improved by combination with other polymers (e.g. dextrin). Alginate membrane should be developed as an alternative to artificial polymer membranes.

Acknowledgements

Sodium alginate samples I-2M and I-2G were kindly provided by KIMICA Corporation (Tokyo, Japan). Professor Hirosi Anzai of Nihon University kindly provided much useful advice for determining the F_{GG} in sodium alginate. Dr. Naoto Arai of Nihon University kindly provided technical advice for SPM observation. Dr. Kei Tao of Nihon University kindly provided technical support of instruments. The authors are grateful to them.

Author details

Keita Kashima and Masanao Imai*

*Address all correspondence to: XLT05104@nifty.com

Course in Bioresource Utilization Sciences, Graduate School of Bioresource Sciences, Nihon University, Japan

References

[1] Sokolnicki, A. M., Fisher, R. J., Harrah, T. P., & Kaplan, D. L. (2006). Permeability of bacterial cellulose membranes. *J. of Membrane Science*, 272, 15-27.

[2] Zhao, M., Xu, X-L., Jiang, Y-D., Sun, W-Z., Wang, W-F., & Yuan, L-M. (2009). Enantioseparation of trans-stilbene oxide using a cellulose acetate membrane. *J. of Membrane Science*, 336, 149-153.

[3] Bigi, A., Cojazzi, G., Panazavolta, S., Roveri, N., & Rubini, K. (2002). Stabilization of gelatin films by crosslinking with genipin. *Biomaterials*, 23, 4827-4832.

[4] Takahashi, T., Imai, M., & Suzuki, I. (2007). Water permeability of chitosan membrane involved in deacetylation degree control. *Biochemical Engineering J.*, 36, 43-48.

[5] Vörösmarty, C. J., Green, P., Salisbury, J., & Lammers, R. B. (2000). Global Water Resources: Vulnerability from Climate Change and Population Growth. *Science*, 289, 284-288.

[6] Gilau, A. M., & Small, M. J. (2008). Designing Cost-Effective Sea Water Reverse Osmosis System under Optimal Energy. *Renewable Energy*, 33, 617-630.

[7] Charcosset, C. (2009). A review of membrane processes and renewable energies for desalination. *Desalination*, 245, 214-231.

[8] Hsu, S. T., Cheng, K. T., & Chiou, J. S. (2002). Seawater desalination by direct contact membrane distillation. *Desalination*, 143, 279-287.

[9] Peng, P., Fane, A. G., & Li, X. (2005). Desalination by membrane distillation adopting a hydrophilic membrane. *Desalination*, 173, 45-54.

[10] Gazagnes, L., Cerneaux, S., Persin, M., Prouzet, E., & Larbot, A. (2007). Desalination of sodium chloride solutions and seawater with hydrophobic ceramic membranes. *Desalination*, 217, 260-266.

[11] Ye, Y., Clech, P. L., Chen, V., Fane, A. G., & Jefferson, B. (2005). Fouling mechanisms of alginate solutions as model extracellular polymeric substances. *Desalination*, 175, 7-20.

[12] Katsoufidou, K., Yiantsios, S. G., & Karabelas, A. J. (2008). An experimental study of UF membrane fouling by humic acid and sodium alginate solutions: the effect of backwashing on flux recovery. *Desalination*, 220, 214-227.

[13] Kashima, K., Imai, M., & Suzuki, I. (2009). Molecular sieving character of calcium alginate membrane relate with polymeric framework and mechanical strength. *J. Bioscience and Bioengineering*, 108, 69.

[14] Papageorgiou, S. K., Katsaros, F. K., Favvas, E. P., Romanos, G. E., Athanasekou, C. P., Beltsios, K. G., Tzialla, O. I., & Falaras, P. (2012). Alginate fibers as photocatalyst immobilizing agents applied in hybrid photocatalytic/ultrafiltration water treatment processes. *Water Research*, 46, 1858-1872.

[15] Takahashi, T., Imai, M., Suzuki, I., & Sawai, J. (2008). Growth inhibitory effect on bacteria of chitosan membranes regulated with deacetylation degree. *Biochemical Engineering J.*, 40, 485-491.

[16] Miao, J., Chen, G., Gao, C., & Dong, S. (2008). Preparation and characterization of N,O-carboxymethyl chitosan/Polysulfone composite nanofiltration membrane cross-linked with epichlorohydrin. *Desalination*, 233, 147-156.

[17] Padaki, M., Isloor, A. M., Fernandes, J., & Prabhu, K. N. (2011). New polypropylene supported chitosan NF-membrane for desalination application. *Desalination*, 280, 419-423.

[18] Haddad, R., Ferjani, E., Roudesli, M. S., & Deratani, A. (2004). Properties of cellulose acetate nanofiltration membranes. Application to brackish water desalination. *Desalination*, 167, 403-409.

[19] Zhang, S., Wang, K. Y., Chung, T-S., Jean, Y. C., & Chen, H. (2011). Molecular design of the cellulose ester-based forward osmosis membranes for desalination. *Chemical Engineering Science*, 66, 2008-2018.

[20] Semiat, R. (2008). Energy issues in desalination processes. *Environmental Science & Technology*, 42, 8193-8201.

[21] Stanford, E. C. C. (1881). British Patent: 142.

[22] Cottrell, I. W., & Kovacs, P. (1980). Alginate. Davidson R T, editor, *Handbook of Water-Soluble Gums and Resins*, United States of America, McGraw-Hill, Inc., 2-1-2-43.

[23] Julian, T. N., Radebaugh, G. W., & Wisniewski, S. J. (1988). Permeability characteristics of calcium alginate films. *J. Controlled Release*, 7, 165-169.

[24] Gacesa, P. Alginates. 1988, *Carbohydrate Polymers*, 8, 161-182.

[25] Lee, S., Ang, W. S., & Elimelech, M. (2006). Fouling of reverse osmosis membranes by hydrophilic organic matter: implications for water reuse. *Desalination*, 187, 313-321.

[26] Ang, W. S., Lee, S., & Elimelech, M. (2006). Chemical and physical aspects of cleaning of organic-fouled reverse osmosis membranes. *J. Membrane Science*, 272, 198-210.

[27] Lee, S., & Elimelech, M. (2006). Relating organic fouling of reverse osmosis membranes to intermolecular adhesion forces. *Environmental Science & Technology*, 40(3), 980-987.

[28] Haug, A., Larsen, B., & Smidsrød, O. (1974). Uronic acid sequence in alginate from different sourcese. *Carbohydrate Research*, 32, 217-225.

[29] Atkins, E. D. T., Nieduszynski, I. A., Mackie, W., Parker, K. D., & Smolko, E. E. (1973). Structural components of alginic acid. I. The crystalline structure of Poly-β-D-mannuronic acid. Results of X-Ray diffraction and polarized infrared studies. *Biopolymers*, 12, 1865-1878.

[30] Atkins, E. D. T., Nieduszynski, I. A., Mackie, W., Parker, K. D., & Smolko, E. E. (1973). Structural components of alginic acid. II. The crystalline structure of Poly-α-L-guluronic. Results of X-Ray diffraction and polarized infrared studies. *Biopolymers*, 12, 1879-1887.

[31] Campa, C., Holtan, S., Nilsen, N., Bjerkan, T. M., Stokke, B. T., & Skjåk-bræk, G. (2004). Biochemical analysis of the processive mechanism for epimerization of alginate by mannuronan C-5 epimerase AlgE4. *Biochemical J.*, 381, 155-164.

[32] Donati, I., Holtan, S., Mørch, Y. A., Borgogna, M., Dentini, M., & Skjåk-bræk, G. (2005). New Hypothesis on the Role of Alternating Sequences in Calcium-Alginate Gels. *Biomacromolecules*, 6, 1031-1040.

[33] Strand, B. L., Mørch, Y. A., Syvertsen, K. R., Espevik, T., & Skjåk-bræk, G. (2003). Microcapsules made by enzymatically tailored alginate. *J. Biomedical Materials Research*, 64A, 540-550.

[34] Katsoufidou, K., Yiantsios, S. G., & Karabelas, A. J. (2007). Experimental study of ultrafiltration membrane fouling by sodium alginate and flux recovery by backwashing. *J. Membrane Science*, 300, 137-146.

[35] Konsoula, Z., & Liakopoulou-Kyriakides, M. (2006). Starch hydrolysis by the action of an entrapped in alginate capsules α-amylase from Bacillus subtilis. *Process Biochemistry*, 41, 343-349.

[36] Almeida, P. F., & Almeida, A. J. (2004). Cross-linked alginate-gelatine beads: a new matrix for controlled release of pindolol. *J. of Controlled Release*, 97, 431-439.

[37] Becerra, M., Baroli, B., Fadda, A. M., Blanco Me´ndez, J., & Gonza´lez Siso, M. J. (2001). Lactose bioconversion by calcium-alginate immobilization of Kluyveromyces lactis cells. *Enzyme and Microbial Technology*, 29, 506-512.

[38] Milovanovic, A., Bozic, N., & Vujcic, Z. (2007). Cell wall invertase immobilization within calcium alginate beads. *Food Chemistry*, 104, 81-86.

[39] Dembczynski, R., & Jankowski, T. (2000). Characterisation of small molecules diffusion in hydrogel-membrane liquid-core capsules. *Biochemical Engineering J.*, 6, 41-44.

[40] Smidsrød, O., & Haug, A. (1968). Dependence upon Uronic Acid Composition of Some Ion-Exchange Properties of Alginates. *Acta Chemica Scandinavica*, 22, 1989-1997.

[41] Draget, K. I., Smidsrød, O., & Skjåk-Bræk, G. (2000). Alginates from Algae. In: Stenbuchel A, Rhee S K, editors, *Polysaccharides and Polyamides in the Food Industry. Properties, Production and Patents*, Federal Republic of Germany, Wiley-VCH, 1-30.

[42] Grant, G. T., Morris, E. R., Rees, D. A., Smith, P. J. C., & Thom, D. (1973). Biological interactions between polysaccharides and divalent cations: The egg-box model. *FEBS Letters*, 32, 195-198.

[43] Kvam, B. J., Grasdalen, H., Smidsrød, O., & Anthonsen, T. (1986). NMR Studies of the Interaction of Metal Ions with Poly(1,4-hexuronates). VI. Lanthanide(III) Complexes of Sodium (Methyl alpha-D-galactopyranosid) uronate and Sodium (Phenylmethyl alpha-D-galactopyranosid) uronate. *Acta Chemica Scandinavica*, B40, 735-739.

[44] Sossna, M., Hollas, M., Schaper, J., & Scheper, T. (2007). Structural development of asymmetric cellulose acetate microfiltration membranes prepared by a single-layer dry-casting method. *J. of Membrane Science*, 289, 7-14.

[45] Takahashi, T., Imai, M., & Suzuki, I. (2008). Cellular structure in an N-acetyl-chitosan membrane regulate water permeability. *Biochemical Engineering J.*, 42, 20-27.

[46] Teixeira, J. A., Mota, M., & Venancio, A. (1994). Model identification and diffusion coefficients determination of glucose and malic acid in calcium alginate membranes. *The Chemical Engineering J.*, 56, B9-B14.

[47] Zhang, W., & Franco, C. M. M. (1999). Critical assessment of quasi-steady-state method to determine effective diffusivities in alginate gel membranes. *Biochemical Engineering J.*, 4, 55-63.

[48] Grassi, M., Colombo, I., & Lapasin, R. (2001). Experimental determination of the theophylline diffusion coefficient in swollen sodium-alginate membranes. *J. Controlled Release*, 76, 93-105.

[49] Hubble, J., & Newman, J. D. (1985). Alginate Ultrafiltration Membranes. *Biotechnology Letters*, 7(4), 273-276.

[50] Andreopoulos, A. G. (1987). Diffusion characteristics of alginate membranes. *Biomaterials*, 8, 397-400.

[51] Aslani, P., & Kennedy, R. A. (1996). Studies on diffusion in alginate gels. I. Effect of cross-linking with calcium or zinc ions on diffusion of acetaminophen. *J. Controlled Release*, 42, 75-82.

[52] Zimmermann, H., Wählisch, F., Baier, C., Westhoff, M., Reuss, R., Zimmermann, D., Behringer, M., Ehrhart, F., Katsen-Globa, A., Giese, C., Marx, U., Sukhorukov, V. L., Vásquez, J. A., Jakob, P., Shirley, S. G., & Zimmermann, U. (2007). Physical and biological properties of barium cross-linked alginate membranes. *Biomaterials*, 28, 1327-1345.

[53] Toti, U. S., & Aminabhavi, T. M. (2004). Different viscosity grade sodium alginate and modified sodium alginate membranes in pervaporation separation of water + acetic acid and water + isopropanol mixtures. *J. of Membrane Science*, 228, 199-208.

[54] Yeom, C. K., & Lee, K-H. (1998). Characterization of Sodium Alginate Membrane Crosslinked with Glutaraldehyde in Pervaporation Separation. *J. of Applied Polymer Science*, 67, 209-219.

[55] Kalyani, S., Smitha, B., Sridhar, S., & Krishnaiah, A. (2008). Pervaporation separation of ethanol-water mixtures through sodium alginate membranes. *Desalination*, 229, 68-81.

[56] Yang, G., Zhang, L., Peng, T., & Zhong, W. (2000). Effects of Ca^{2+} bridge cross-linking on structure and pervaporation of cellulose/alginate blend membranes. *J. of Membrane Science*, 175, 53-60.

[57] Chen, J. H., Ni, J. C., Liu, Q. L., & Li, S. X. (2012). Adsorption behavior of Cd(II) ions on humic acid-immobilized sodium alginate and hydroxyl ethyl cellulose blending porous composite membrane adsorbent. *Desalination*, 285, 54-61.

[58] Saraswathi, M., Rao, K. M., Prabhakar, M. N., Prasad, C. V., Sudakar, K., Naveen Kumar, H. M. P., Prasad, M., Rao, K. C., & Subha, M. C. S. (2011). Pervaporation studies of sodium alginate (SA)/dextrin blend membranes for separation of water and isopropanol mixture. *Desalination*, 269, 177-183.

[59] Wang, X. P. (2000). Modified alginate composite membranes for the dehydration of acetic acid. *J. of Membrane Science*, 170, 71-79.

[60] Kanti, P., Srigowri, K., Madhuri, J., Smitha, B., & Sridhar, S. (2004). Dehydration of ethanol through blend membranes of chitosan and sodium alginate by pervaporation. *Separation and Purification Technology*, 40, 259-266.

[61] Reddy, A. S., Kalyani, S., Kumar, N. S., Boddu, V. M., & Krishnaiah, A. (2008). Dehydration of 1,4-dioxane by pervaporation using crosslinked calcium alginate-chitosan blend membranes. *Polymer Bulletin*, 61, 779-790.

[62] Smitha, B., Sridhar, S., & Khan, A. A. (2005). Chitosan-sodium alginate polyion complexes as fuel cell membranes. *European Polymer J.*, 41, 1859-1866.

[63] Kashima, K., Imai, M., & Suzuki, I. (2010). Superior molecular size screening and mass-transfer characterization of calcium alginate membrane. *Desalination and Water Treatment*, 17, 143-149.

[64] Li, Y., Hu, M., Du, Y., Xao, H., & McClements, D. J. (2011). Control of lipase digestibility of emulsified lipids by encapsulation within calcium alginate beads. *Food Hydrocolloids*, 25, 122-130.

[65] Kashima, K., & Imai, M. (2011). Dominant impact of the α-L-guluronic acid chain on regulation of the mass transfer character of calcium alginate membranes. *Desalination and Water Treatment*, 34, 257-265.

[66] Bitter, T., & Muir, H. M. (1962). A modified uronic acid carbazole reaction. *Analytical Biochemistry*, 4, 330-334.

[67] Anzai, H., Uchida, N., & Nishide, E. (1986). Comparative studies of colorimetric analysis for uronic acids. *Bull. Coll. Agr. & Vet. Med., Nihon Univ.*, 43, 53-56.

[68] Benavides, S., Villalobos-Carvajal, R., & Reyes, J. E. (2012). Physical, mechanical and antibacterial properties of alginate film: Effect of the crosslinking degree and oregano essential oil concentration. *J. Food Engineering*, 110, 232-239.

[69] Rhim, J-W. (2004). Physical and mechanical properties of water resistant sodium alginate films. *Lebensmittel-Wissenschaft und-Technologie*, 37, 323-330.

[70] Olivas, G. I., & Barbosa-Canovas, G. V. Alginate-calcium films: Water vapor permeability and mechanical properties as affected by plasticizer and relative humidity. 2008, *LWT- Food Science and Technology*, 41, 359-366.

[71] Boricha, A. G., & Murthy, Z. V. P. (2010). Preparation of N,O-carboxymethyl chitosan/cellulose acetate blend nanofiltration membrane and testing its performance in treating industrial wastewater. *Chemical Engineering Journal*, 157, 393-400.

[72] Huang, Q-L., Xiao, C-F., Hu, X-Y., & Li, X-F. (2011). Study on the effects and properties of hydrophobic poly(tetrafluoroethylene) membrane. *Desalination*, 277, 187-192.

[73] Schwarz, H-H., & Hicke, H-G. (1989). Influence of Casting Solution Concentration on Structure and Performance of Cellulose Acetate Membranes. *J. Membrane Science*, 46, 325-334.

[74] So, M. T., Eirich, F. R., Strathmann, H., & Baker, R. W. (1973). Preparation of Asymmetric Loeb-sourirajan Membranes. *J. Polymer Science: Polymer Letters Edition*, 11, 201-205.

[75] Block, W. (2003). Water status and thermal analysis of alginate beads used in cryopreservation of plant germplasm. *Cryobiology*, 47, 59-72.

[76] Al-Rub, F. A. A., Banat, F., & Beni-Melhim, K. (2002). Parametric sensitivity analysis of direct contact membrane distillation. *Separation Science and Technology*, 37(14), 3245-3271.

[77] Adnan, S., Hoang, M., Wang, H., & Xie, Z. (2012). Commercial PTFE membranes for membrane distillation application: Effect of microstructure and support material. *Desalination*, 284, 297-308.

[78] Wu, P., & Imai, M. (2011). Food polymer pullulan-κ-carrageenan composite membrane performed smart function both on mass transfer and molecular size recognition. *Desalination and Water Treatment*, 34, 239-245.

[79] Yasuda, H., Lamaze, C. E., & Peterlin, A. (1971). Diffusive and hydraulic permeabilities of water in water-swollen polymer membranes. *J. Polymer Science: Part A-2*, 9, 1117-1131.

[80] Wilke, C. R., & Chang, P. (1955). Correlation of Diffusion Coefficients in Dilute Solutions. *AIChE J.*, 1, 264-270.

[81] Chen, S. X., & Lostritto, R. T. (1996). Diffusion of benzocaine in poly (ethylene-vinyl acetate) membranes: Effects of vehicle ethanol concentration and membrane vinyl acetate content. *J. Controlled Release*, 38, 185-191.

[82] Vadalkar, V. S., Kulkarni, M. G., & Bhagwat, S. S. (1993). Anomalous sorption of binary solvents in glassy polymers: interpretation of solute release at constant rates. *Polymer*, 34, 4300-4306.

[83] Baker, R. W. (2004). *Membrane Technology and Applications*, England, John Wiley & Sons, Ltd., 67-68.

[84] Mehmetoglu, U. (1990). Effective diffusion coefficient of sucrose in calcium alginate gel. *Enzyme Microbial Technology*, 12, 124-126.

[85] Longo, M. A., Novella, I. S., Garcia, L. A., & Diaz, M. (1992). Diffusion of proteases in calcium alginate beads. *Enzyme and Microbial Technology*, 14, 586-590.

[86] Kikuchi, A., Kawabuchi, M., Watanabe, A., Sugihara, M., Sakurai, Y., & Okano, T. (1999). Effect of Ca^{2+}-alginate gel dissolution on release of dextran with different molecular weights. *J. Controlled Release*, 58, 21-28.

[87] Koyama, K., & Seki, M. (2004). Evaluation of Mass-Transfer Characteristics in Alginate-Membrane Liquid-Core Capsules Prepared Using Polyethylene Glycol. *J. Bioscience and Bioengineering*, 98, 114-121.

[88] Merdaw, A. A., Sharif, A. O., & Derwish, G. A. W. (2010). Water permeability in polymeric membranes, Part I. *Desalination*, 260, 180-192.

[89] Cho, C. H., Oh, K. Y., Kim, S. K., Yeo, J. G., & Sharma, P. (2011). Pervaporative seawater desalination using NaA zeolite membrane: Mechanisms of high water flux and high salt rejection. *J. Membrane Science*, 371, 226-238.

[90] Hsieh, K. H., Lin, B. Y., & Chiu, W. Y. (1989). Studies on Diisocyanate-Modified Cellulose Acetate Membranes. *Desalination*, 71, 97-105.

[91] Saljoughi, E., Sadrzadeh, M., & Mohammadi, T. (2009). Effect of preparation variables on morphology and pure water permeation flux through asymmetric cellulose acetate membranes. *J Membrane Science*, 326, 627-634.

[92] Claes, S., Vandezande, P., Mullens, S., Leysen, R., De Sitter, K., Andersson, A., Maurer, F. H. J., Van den Rul, H., Peeters, R., & Van Bael, M. K. (2010). Pervaporation separation of water + isopropanol mixtures using novel nanocomposite membranes of poly(vinyl alcohol) and polyaniline. *J Membrane Science*, 351, 160-167.

[93] Kurkuri, M. D., Toti, U. S., & Aminabhavi, T. M. (2002). Syntheses and Characterization of Blend Membranes of Sodium Alginate and Poly(vinyl alcohol) for the Pervaporation Separation of Water + Isopropanol Mixtures. *J Applied Polymer Science*, 86, 3642-3651.

[94] Vijaya Kumar Naidu, B., Sairam, M., Raju, K. V. S. N., & Aminabhavi, T. M. (2005). High flux composite PTMSP-silica nanohybrid membranes for the pervaporation of ethanol/water mixtures. *J. Membrane Science*, 260, 142-155.